Analysing and combining atmospheric general circulation model simulations forced by prescribed SST: northern extratropical response

Vincent Moron ([1]), **Antonio Navarra** ([2]), **M. Neil Ward** ([3]), **Chris K. Folland** ([4]), **Petra Friederichs** ([5]), **Karine Maynard** ([6]) **and Jan Polcher** ([6])

([1]) *UFR des Sciences Géographiques et de l'Aménagement, Université de Provence and UMR CEREGE, CNRS, Aix en Provence, France*

([2]) *Istituto Nazionale di Geofisica e Vulcanologia, Bologna, Italy*

([3]) *CIMMS, University of Oklahoma, Norman, U.S.A.*

([4]) *Hadley Centre for Climate Prediction and Research, Meteorological Office, Bracknell, England*

([5]) *Meteorologisches Institut des Universitaet Bonn, Germany*

([6]) *LMD-CNRS, Université Pierre et Marie Curie, Paris, France*

Abstract

The ECHAM 3.2 (T21), ECHAM 4 (T30) and LMD (version 6, grid-point resolution with 96 longitudes × 72 latitudes) atmospheric general circulation models were integrated through the period 1961 to 1993 forced with the same observed Sea Surface Temperatures (SSTs) as compiled at the Hadley Centre. Three runs were made for each model starting from different initial conditions. The mid-latitude circulation pattern which maximises the covariance between the simulation and the observations, *i.e.* the most skilful mode, and the one which maximises the covariance amongst the runs, *i.e.* the most reproducible mode, is calculated as the leading mode of a Singular Value Decomposition (SVD) analysis of observed and simulated Sea Level Pressure (SLP) and geopotential height at 500 hPa (Z500) seasonal anomalies. A common response amongst the different models, having different resolution and parametrization should be considered as a more robust atmospheric response to SST than the same response obtained with only one model. A robust skilful mode is found mainly in December-February (DJF), and in June-August (JJA). In DJF, this mode is close to the SST-forced pattern found by Straus and Shukla (2000) over the North Pacific and North America with a wavy out-of-phase between the NE Pacific and the SE US on the one hand and the NE North America on the other. This pattern evolves in a NAO-like pattern over the North Atlantic and Europe (SLP) and in a more N-S tripole on the Atlantic and European sector with an out-of-phase between the middle Europe on the one hand and the northern and southern parts on the other (Z500). There are almost no spatial shifts between either field around North America (just a slight eastward shift of the highest absolute heterogeneous correlations for SLP relative to the Z500 ones). The time evolution of the SST-forced mode is moderatly to strongly related to the ENSO/LNSO events but the spread amongst the ensemble of runs is not systematically related at all to the intensity of Niño3.4 SST anomalies. The leading reproducible mode in JJA is clearer and more skilful for SLP than for Z500 and also seems related to the SST time evolution of tropical Pacific. It is characterised by an out-of-phase between the whole North Pacific and a horseshoe shaped area from Eastern Siberia and Gulf of Mexico. The leading OM mode found in MAM and SON, are quite close to the DJF one (at least for the modelled anomalies), but they are less skilful than in DJF. The most skilful mode (*i.e.* SLP-Z500 mode in DJF and SLP mode in JJA) is almost similar to the most reproducible one during these particular seasons. In MAM and SON, the SST-forced pattern is very close to the wintertime one. The warm episodes in the central and eastern tropical Pacific are then associated with negative pressure anomalies at the sea level and also at 500 hPa over the whole North Pacifkc and from SE US Coast to Western Europe (from SE US Coast to Scandinavia for Z500) and positive pressure anomalies on Central Canada, north of 55°-60°N across the North Atlantic and also over Northern Siberia (in MAM). The variance forced by SST are lower in MAM and SON than in DJF and, as suggested above, the skill of this SST-forced mode is weak in MAM and almost close to zero in SON.

Mailing address: Dr. Antonio Navarra, Istituto Nazionale di Geofisica e Vulcanologia, Viale Carlo Berti Pichat 8, 40127 Bologna, Italy; e-mail: navarra@ingv.it

Key words *atmospheric general circulation model – inter-comparison – northern hemisphere – seasonal anomalies – tropical Pacific SST*

1. Introduction

The extratropical atmospheric response to local and/or global Sea Surface Temperature (SST) anomalies is less clear (*i.e.* Zorita *et al.*, 1992; Lau, 1997) than the tropical ones (see Moron *et al.*, 2001). Many diagnostic studies stated that wintertime monthly and seasonal SST anomalies in the mid-latitude ocean are correlated with large-scale quasi-stationary atmospheric perturbations and concluded that the atmosphere leads the ocean on seasonal and annual time scales linked to local air-sea interaction (*i.e.* Bjerknes, 1964; Davis, 1976; Zorita *et al.*, 1992; Wallace *et al.*, 1990, 1992). Saranavan (1998) found from various coupled integrations that the dominant modes of interannual SST anomalies variability in the North Pacific and North Atlantic ocean are forced by the corresponding dominant modes of atmospheric low-frequency variability, namely the Pacific-North America (hereafter PNA) and the North Atlantic Oscillation (hereafter NAO) (see also Verbeek, 1997 for the North Atlantic). PNA and NAO-like patterns also occur in integrations without any interannual SST variations, indicating that they are indeed natural modes of uncoupled atmospheric variability. The specification of air-sea coupling does not crudely modify the pattern, but changes the variance of these modes (Saranavan, 1998). The main ocean-atmospheric patterns at decadal and longer time scales seem not directly linked to local air-sea interaction, and ocean dynamics are important at these timescales (*i.e.* Zorita and Frankignoul, 1997; Grötzner *et al.*, 1998).

Another important issue is the association between tropical SST and extratropical response (*i.e.* Lau and Nath, 1994, 1996; Graham *et al.*, 1994; Kharin, 1995; Renshaw *et al.*, 1998; Saranavan, 1998; Straus and Shukla, 2000; Shukla *et al.*, 2000). There are numerous diagnostic and numerical studies on the relations between El Niño Southern Oscillation (ENSO) phenomenon and the North American response (*i.e.* Graham *et al.*, 1994; Lau and Nath, 1994, 1996; Livezey *et al.*, 1997; Renshaw *et al.*, 1998). The main conclusions stated that El Niño (EN) forces negative SLP anomalies over NE Pacific and positive SLP anomalies over the Rockies. Straus and Shukla (2000) stated that the SST-forced pattern over the North Pacific and North America differs slightly from the classical PNA pattern, which is considered as an internal mode of the atmospheric variability (see their fig. 11). Such studies are less frequent for the Atlantic and Europe (*i.e.* Fraedrich, 1990; Davies *et al.*, 1997; Feddersen, 2000) or Eurasia. The exact impact of tropical Pacific SSTs on European and Atlantic atmospheric circulation is then unclear. Diagnostic studies of Fraedrich *et al.* (Fraedrich, 1990, 1993; Fraedrich and Muller, 1992; Fraedrich *et al.*, 1992) stated that cyclonicity (resp. anticyclonicty) is strongest over Western and Central Europe during EN (resp. la Niña (LN)) winters. Moron and Ward (1998) reviewed the relations and showed that the common variance between sea level pressure over Europe and Niño 3.4 reaches at maximum 15-20% in spring. Studies relating the tropical Atlantic and Europe are rare and not conclusive about the real impact of tropical Atlantic SSTA on European variability (Dequé and Servain, 1989). It also seems that the tropical Pacific influences more strongly extratropical circulation than the tropical Atlantic, partly due to the highest amplitudes of SST anomalies in the first basin.

So it seems from previous studies that extratropical response to local or tropical SST is less reproducible and that the SST-forced component is weaker than for the tropics. This is especially true over the North Atlantic and European sectors. It is then very important to compare different models using the same boundary forcing but including different parametrization schemes to delineate clearly the response of extratropics to global SST forcing (Liang *et al.*, 1997; Barnett *et al.*, 1997; Krishnamurti *et al.*, 2000). We use the same methodology as in Ward and Navarra (1997) and Moron *et al.* (1998) which considered only the response of tropical rainfall in ECHAM 4.0 (se also Moron *et al.*, 2001) to extract the most skilful and reproducible modes of SLP and geopotential height at 500 hPa (Z500 hereafter). Section 2 presents the climatology of the three models in the northern extratropics. Section 3 presents the leading OM mode, which maximises the skill between observations and simulations, and Section 4 the

leading MM mode which maximises the reproducibility between the runs (see Moron *et al.*, 2001 for a description of the methodology). A discussion (Section 5) closes the paper.

2. Climatology

Figure 1 displays the pattern correlations between the mean climatology of observed (from the global data set elaborated by the UKMO) and simulated SLP between 20 and 80°N (after having interpolated observed data on each model grid). All values are significant at the 0.01 level. Correlations are higher from November to February and in July-August. There are significant decreases of pattern correlations around April-May (except for LMD) and around October. Note that the pattern correlations of a prognostic variable in height as Z500 are always higher than 0.93. In DJF (fig. 2a-d), there is a general agreement of the spatial behavior between the three models and observations, with large continental anticyclones connected to subtropical anticyclones of the Pacific and Azores and deep low pressure systems over the Aleoutian Islands and south off Greenland. The Azores high is displaced over North Africa in EC3 and EC4 relative to observations. The aleoutian low is too low for the three models (mainly for EC3). This is also present in COLA AGCM (Shukla *et al.*, 2000). In MAM (not shown), the spatial agreement is not so high. SLP are correctly simulated over the Atlantic and Europe even if the Azores high is too weak for EC3 and too high for LMD. For the Pacific, the aleoutian low remains too deep in EC3 and EC4. The situation is quite complicated over Eurasia,

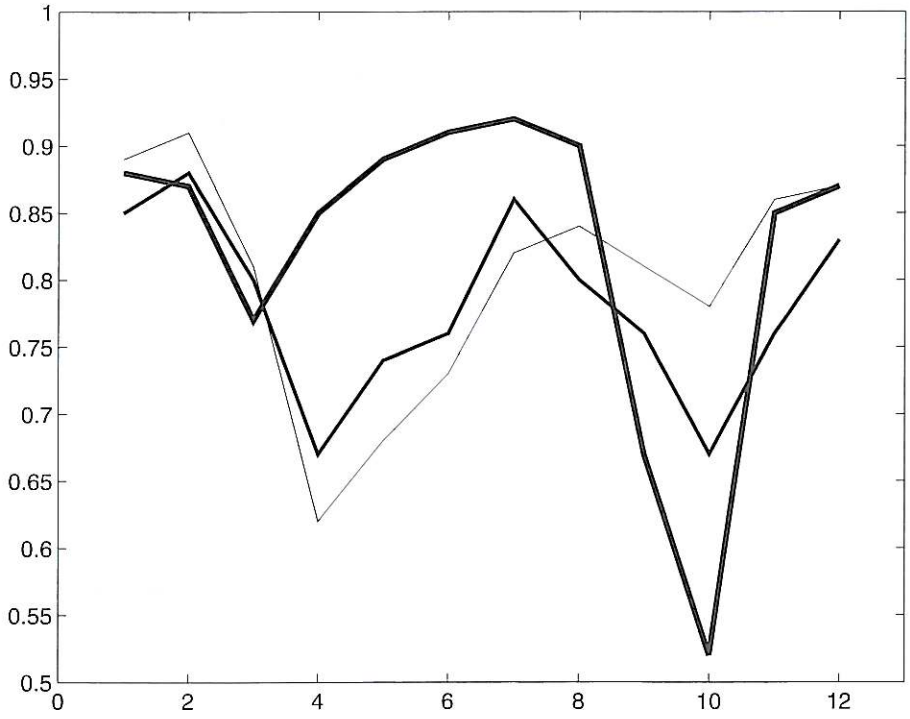

Fig. 1. Monthly pattern correlations between observed and simulated SLP by the three models. Observed data are independently and linearly interpolated on each model grid for computing the pattern correlations. Only data between 20 and 80°N are used.

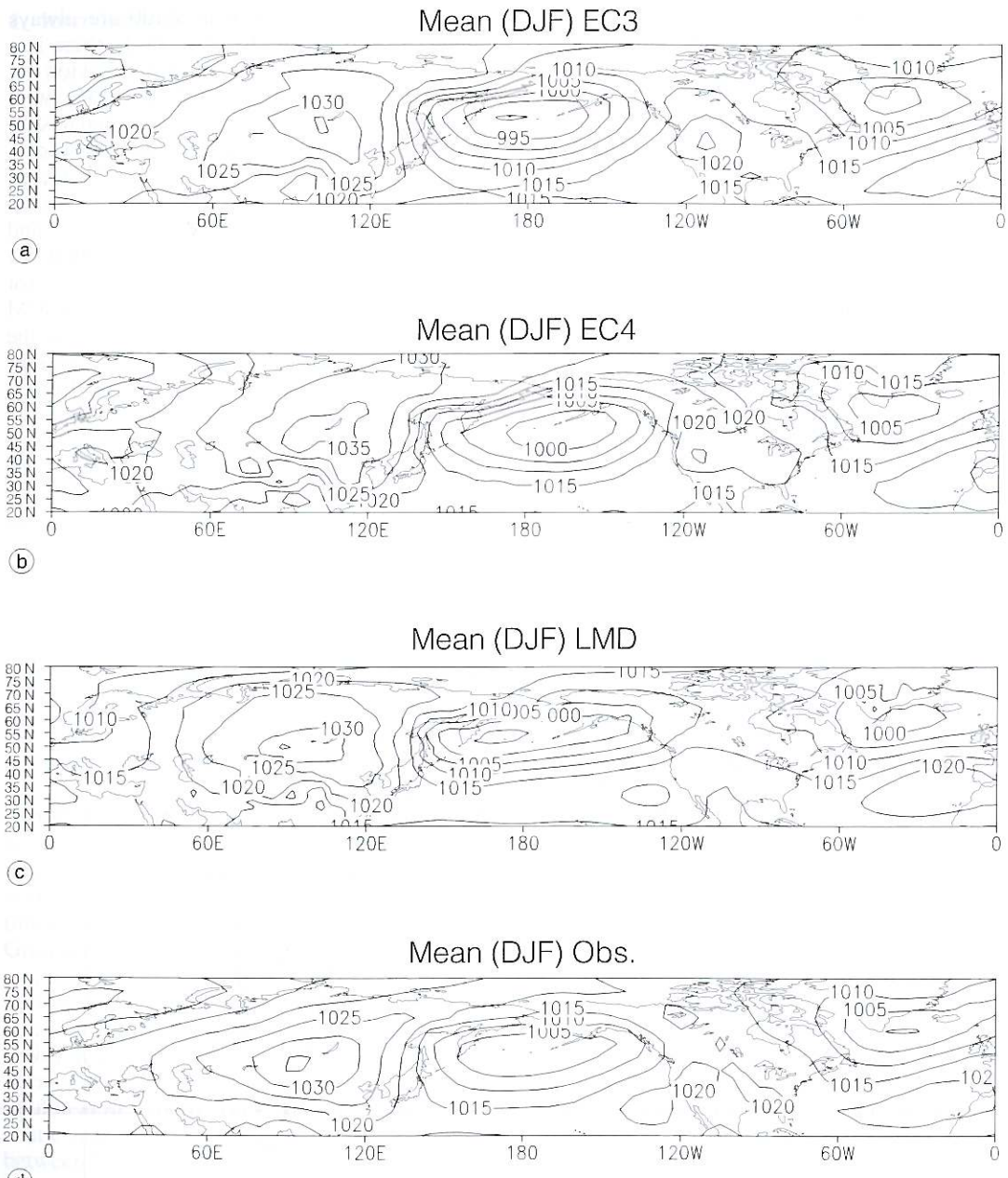

Fig. 2a-d. Seasonal mean of sea level pressure in DJF for: a) EC3; b) EC4; c) LMD; d) observation.

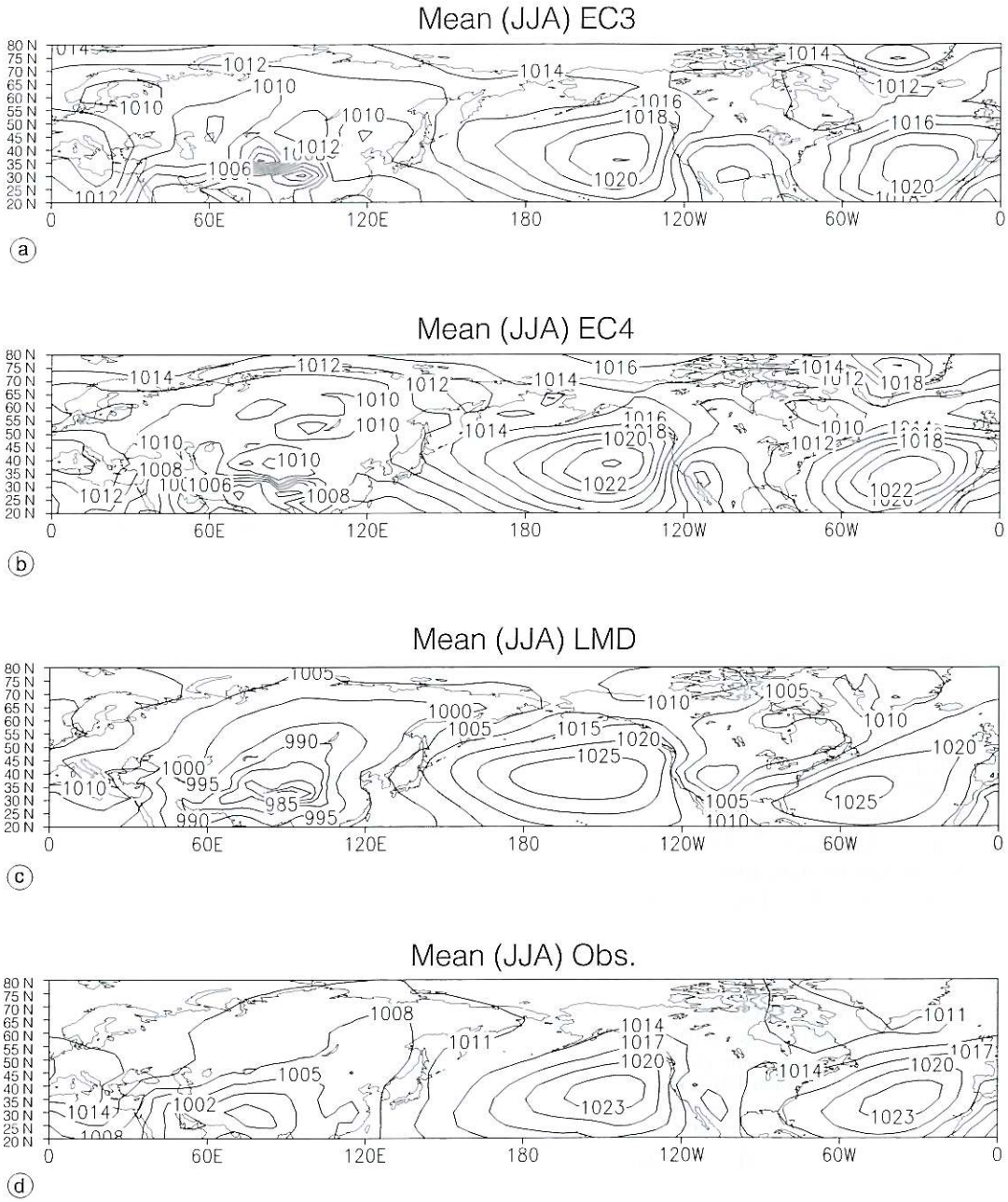

Fig. 3a-d. Same as fig. 2a-d except for JJA.

where the monsoon low appears over Northern India. Such disagreement also occurs in JJA (fig. 3a-d). The magnitude is better simulated by EC3 and EC4, but the spatial pattern remains too complex over the Tibet highs. In SON (not shown), the situation remains complicated between India and Mongolia. The Siberian high appears and is correctly simulated by EC3 and EC4. Its location is too north in LMD. The circulation seems correctly reproduced over the Atlantic and Pacific basins even if the aleoutian low is too deep in EC3 and EC4 integrations. In summary: i) the agreement between observations and model is good for the three models over Atlantic even if EC3 and EC4 displace the Azores high toward North Africa in autumn and winter. Iceland low is also too low mainly for EC3 and LMD; ii) the simulation is also correct for the Pacific and North America even if the aleoutian low is too low in the three models; iii) the main disagreement occurs over Eurasia between spring and autumn.

3. The leading skilful SLP and Z500 mode

In order to determine the dominant OM pattern which maximizes the skill, we employ cross-validated singular value decomposition (Moron *et al.*, 1998, 2001; Feddersen *et al.*, 1999) of the observed and simulated SLP and Z500 (refer to Section 2.3., Moron *et al.*, 2001). The heterogeneous correlations of the four seasons are shown in fig. 4a-d for SLP and fig. 5a-d for Z500.

In DJF, the OM_m pattern of SLP consists of positive values over NE Pacific but also North Atlantic and Europe south of 60°N and weak negative values over Central Canada and North Atlantic and Europe north of 60°N. The heterogeneous correlations are weak over the whole of Asia (fig. 4a). This broad-scale pattern is well matched by the OM_o ones (table I and fig. 4a). The OM_m pattern of Z500 is quite similar to the SLP ones (fig. 5a), but heterogeneous correlations are usually higher, especially from North Pacific to North Atlantic, and the leading OM mode explains a larger fraction of the whole simulated variance (table I). Note that SLP and Z500 OM_m patterns differ slightly over the North Atlantic; the negative heterogenous correlations are more SW-NE elongated from SE US to Scandinavia for Z500 and negative heterogeneous correlations appear over the East Mediterranean area and Middle East (fig. 5a). As for SLP, the OM_o pattern well matches this behavior (table I and fig. 5a). The heterogeneous correlations of OM_o are simply weaker than those of OM_m over the North Atlantic and Europe. The time series associated with the leading OM_m (respectively OM_o) are strongly (respectively moderatly) related to the Niño3.4 index (table II). The difference between the OM_m and OM_o correlations with Niño3.4 could suggest that the ensemble of AGCM used here overestimates the SST forcing linked to EN/LN episodes relative to observations. Another explanation could be the fact that the runs used here consider the only SST forcing and also the simulated internal dynamics

Table I. Summary of OM analysis of the Northern Hemisphere (20-80°N) SLP and Z500. OM_o (%) and OM_m (%) are the variance explained for each field (= weighted mean of the squared heterogeneous correlations). Skill is the cross-correlation between cross-validated observed and simulated time series. The mean of the nine runs is used here. Spatial match is the pattern correlation between OM_o and OM_m (after having linearly interpolated observed data on a common T21 grid).

	SLP				Z500			
	OM_o (%)	OM_m (%)	Skill	Spatial match	OM_o (%)	OM_m (%)	Skill	Spatial match
DJF	10.6	11.1	0.44	0.64	9.9	17.3	0.64	0.62
MAM	6.3	5.7	0.43	0.06	7.7	7.4	0.31	0.40
JJA	9.6	14.8	0.55	0.75	6.6	6.8	0.46	0.56
SON	6.1	6.9	0.26	0.33	5.6	4.1	0.35	0.13

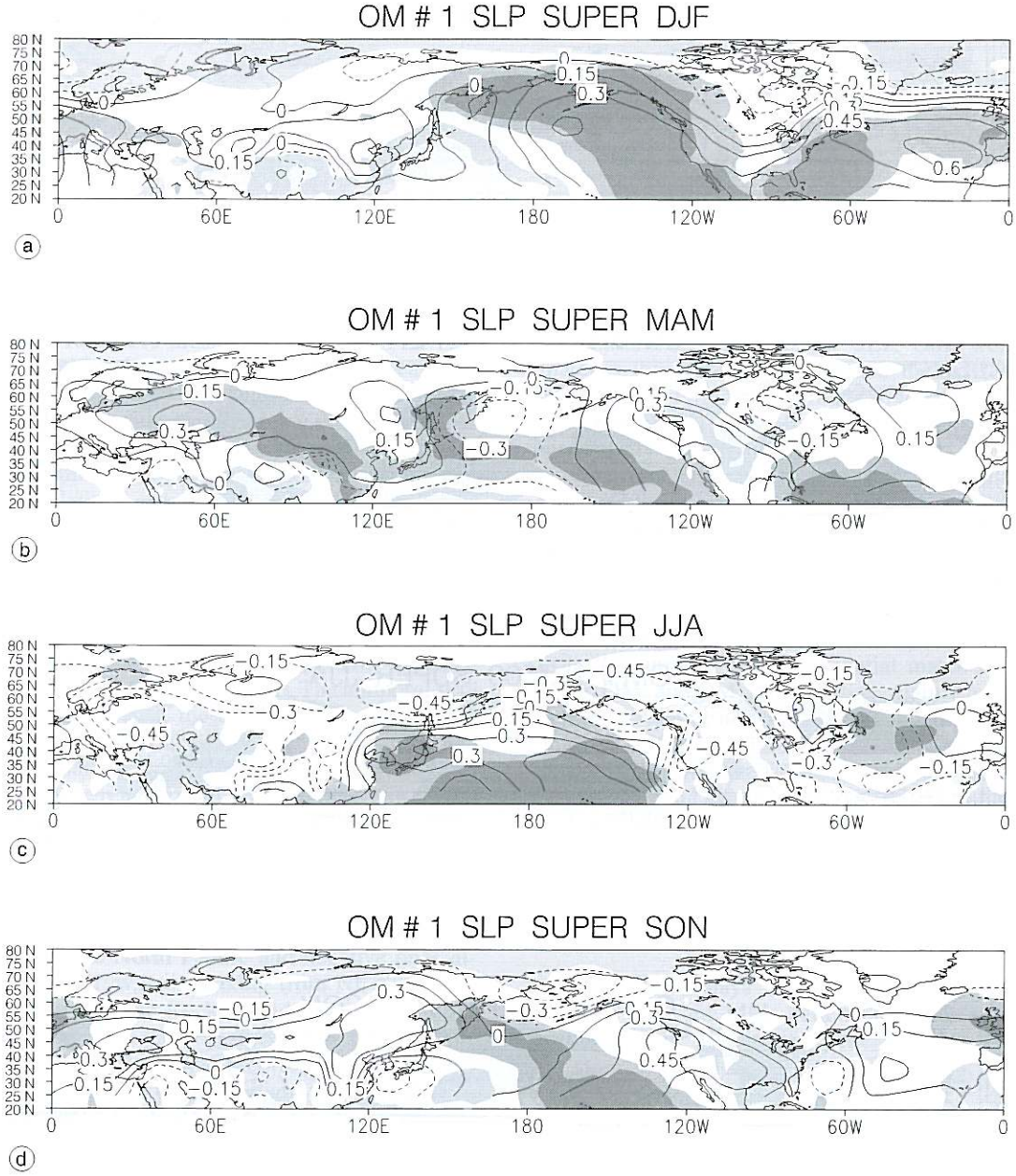

Fig. 4a-d. Heterogeneous correlations pattern in: a) DJF; b) MAM; c) JJA; d) SON super-ensemble North Hemisphere SLP OM analysis. The heterogeneous correlations of OM_o are displayed as shadings (very light grey: below – 0.3; light grey: between – 0.15 and – 0.3; white: between – 0.15 and 0.15; dark grey: between 0.15 and 0.3; very dark grey: over 0.3) and those of OM_m are contoured every 0.15 values with negative values in dotted lines.

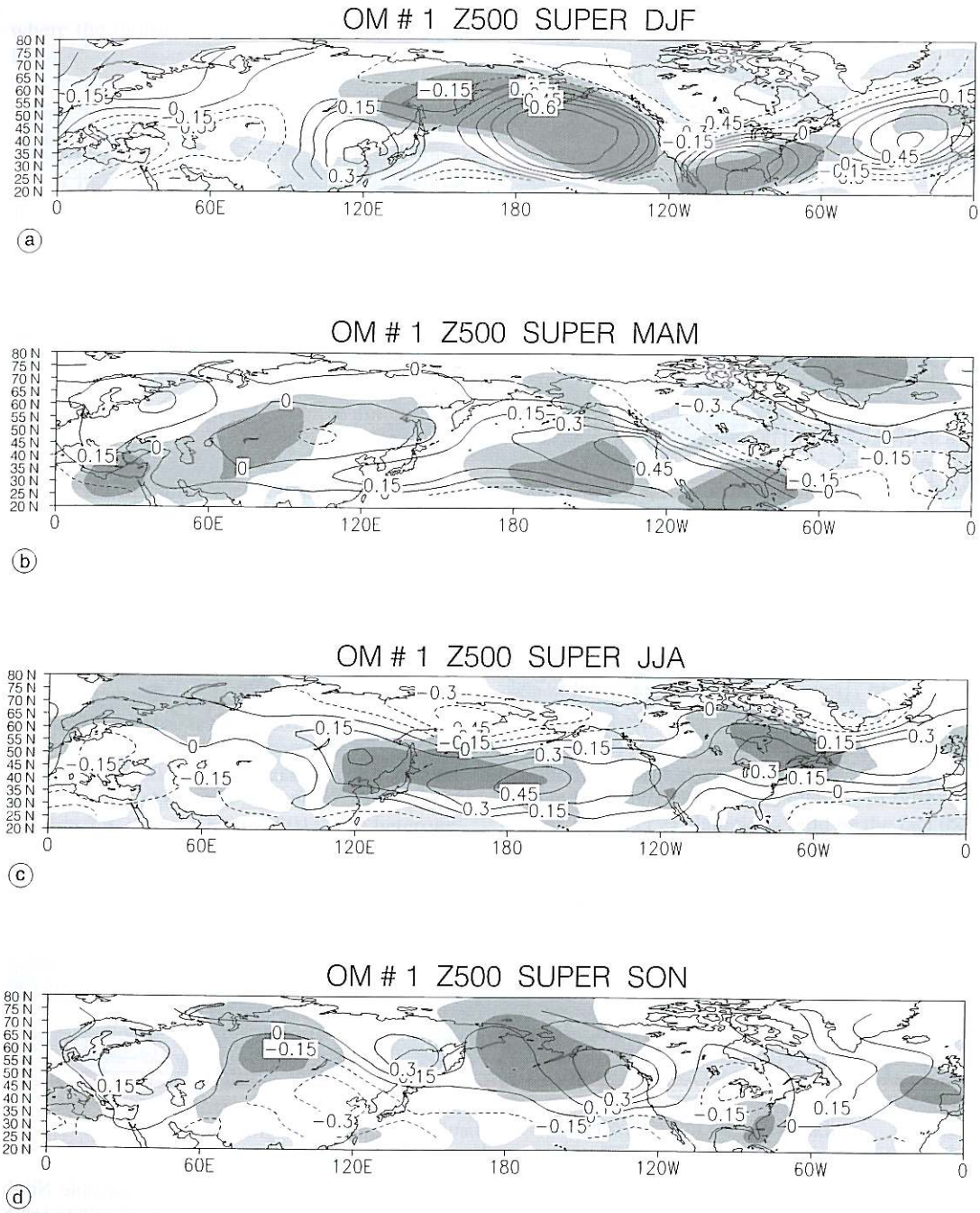

Fig. 5a-d. Same as fig. 4a-d except for Z500.

Table II. Correlations between OM_m and OM_o time series and the Niño3.4 SST index.

	SLP – OM_o	SLP – OM_m	Z500 – OM_o	Z500 – OM_m
DJF	– 0.38	– 0.78	– 0.60	– 0.84
MAM	– 0.47	– 0.62	– 0.50	– 0.75
JJA	– 0.57	– 0.64	– 0.40	– 0.86
SON	– 0.38	– 0.62	– 0.13	– 0.37

while the observations contain other sources of variations and decreases the level of correlations related to the sole SST forcing.

In MAM, the SLP OM_m pattern appears as a residual of the winter one, with weaker heterogeneous correlations, reducing the explained variance (table I and fig. 4b). There is also a 20-30° eastward shift of the highest heterogeneous correlations over the North Pacific and North America relatively to the winter figure, and the North Atlantic values are now close to zero (fig. 4b). The spatial match with OM_o drops close to zero (table I). The leading OM mode of Z500 (fig. 5b) explains a larger fraction of the whole variance, and OM_o and OM_m patterns are more similar than for SLP (fig. 5a). The temporal skill is weak, even if the correlations with Niño3.4 remain strong (table II). Note also that OM_o and OM_m patterns are almost reversed over the North Atlantic, relative to the winter ones (fig. 5a,b). The time series associated with the leading OM mode of SLP and Z500 are strongly correlated (r = 0.78 for OM_o and 0.60 for OM_m).

The leading OM_m pattern of SLP in JJA consists of positive heterogeneous correlations over the whole North Pacific and negative ones almost everywhere, peaking from NE Siberia to Alaska and the Rockies and also over Eastern Europe. This pattern is well matched by OM_o with the highest pattern correlation recorded in table II. The skill is also high (table I) and OM_o and OM_m time series are strongly related to Niño3.4 behavior (table II). In other terms, warm Niño3.4 events are associated with a lowering of SLP over the North Pacific with increasing SLP in a surrounding horse-shoe shaped region from NE Siberia to Alaska and Gulf of Mexico. The leading OM_m pattern of Z500 in JJA is quite different (fig.5c). It consists of a more zonal pattern with positive heterogeneous correlations from Korea-Japan to Newfoundland and Great Britain, surrounded by negative heterogeneous correlations (fig. 5c). As for SLP, OM_o well matches this pattern (table I) and the skill is higher than during the spring (Niño3.4). The time evolution of the leading OM mode remains moderately similar between OM and Z500 (r = 0.46 for OM_o and 0.65 for OM_m), despite the spatial difference between both fields.

The leading OM_m pattern of SLP in SON consists of positive heterogeneous correlations elongated from the Middle East to Western America surrounded by weak negative values (fig. 4d). The skill and explained variance drop strongly from the summer case. The spatial match between OM_o and OM_m is borderline, mainly over the North Atlantic and Eurasia. The leading OM mode of Z500 explains a small fraction of the observed and simulated variance and the spatial match between OM_o and OM_m is very low (table I). This season represents then the worst skill.

4. The leading reproducible SLP and Z500 mode

Table III displays the pattern correlations between OM_m and MM_m patterns and indicates basically if the most skilful pattern is also the

Table III. Pattern correlations between the leading OM_m and MM_m modes.

	SLP	Z500
DJF	0.93	0.97
MAM	– 0.05	0.57
JJA	0.88	0.23
SON	0.59	– 0.18

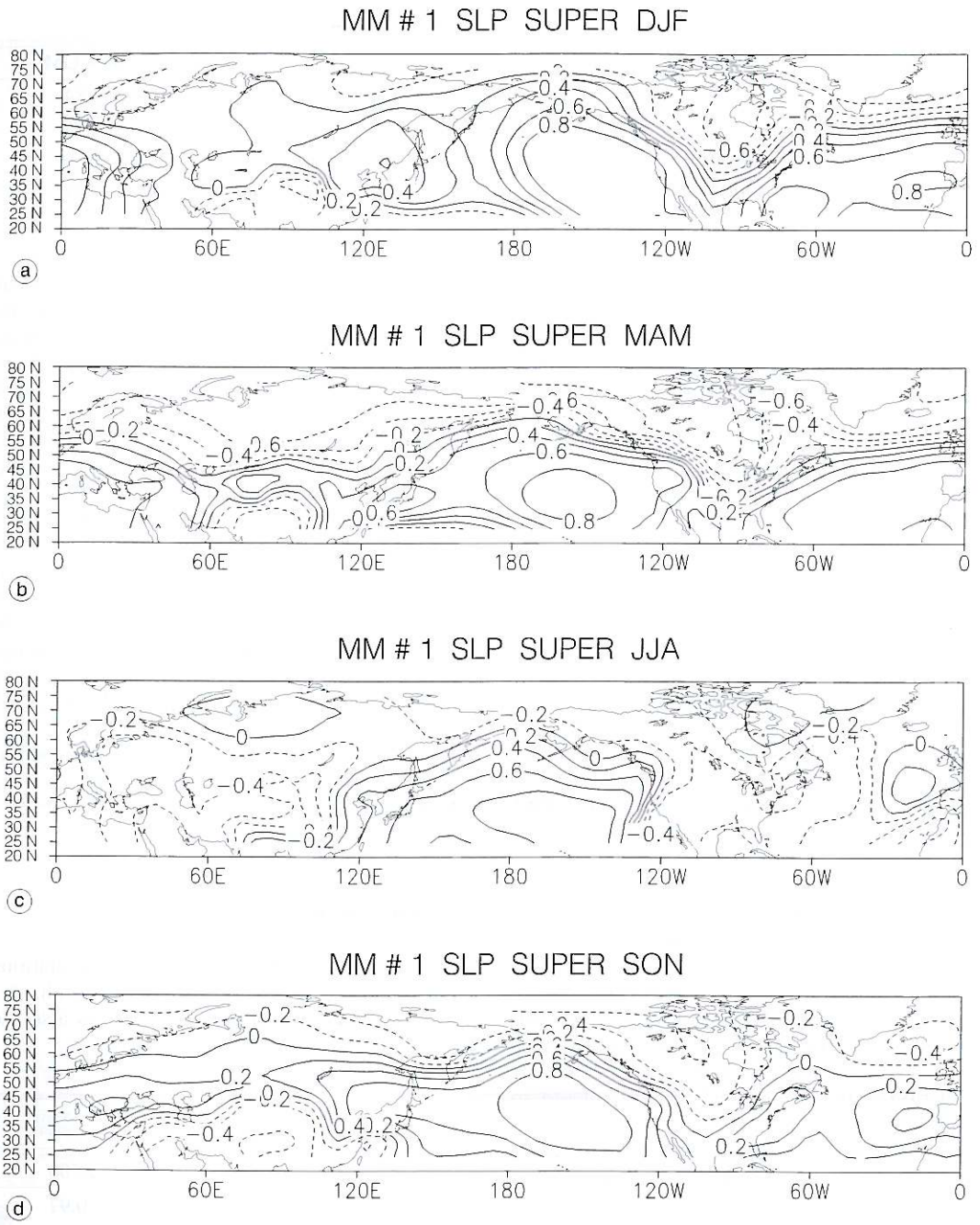

Fig. 6a-d. Same as fig. 4a-d except for the first SVD MM mode of North Hemispheric SLP in: a) DJF; b) MAM; c) JJA; d) SON. The contours are homogeneous correlations between the mean of the cross-validated MM_m time series scores and the mean of the 9 runs.

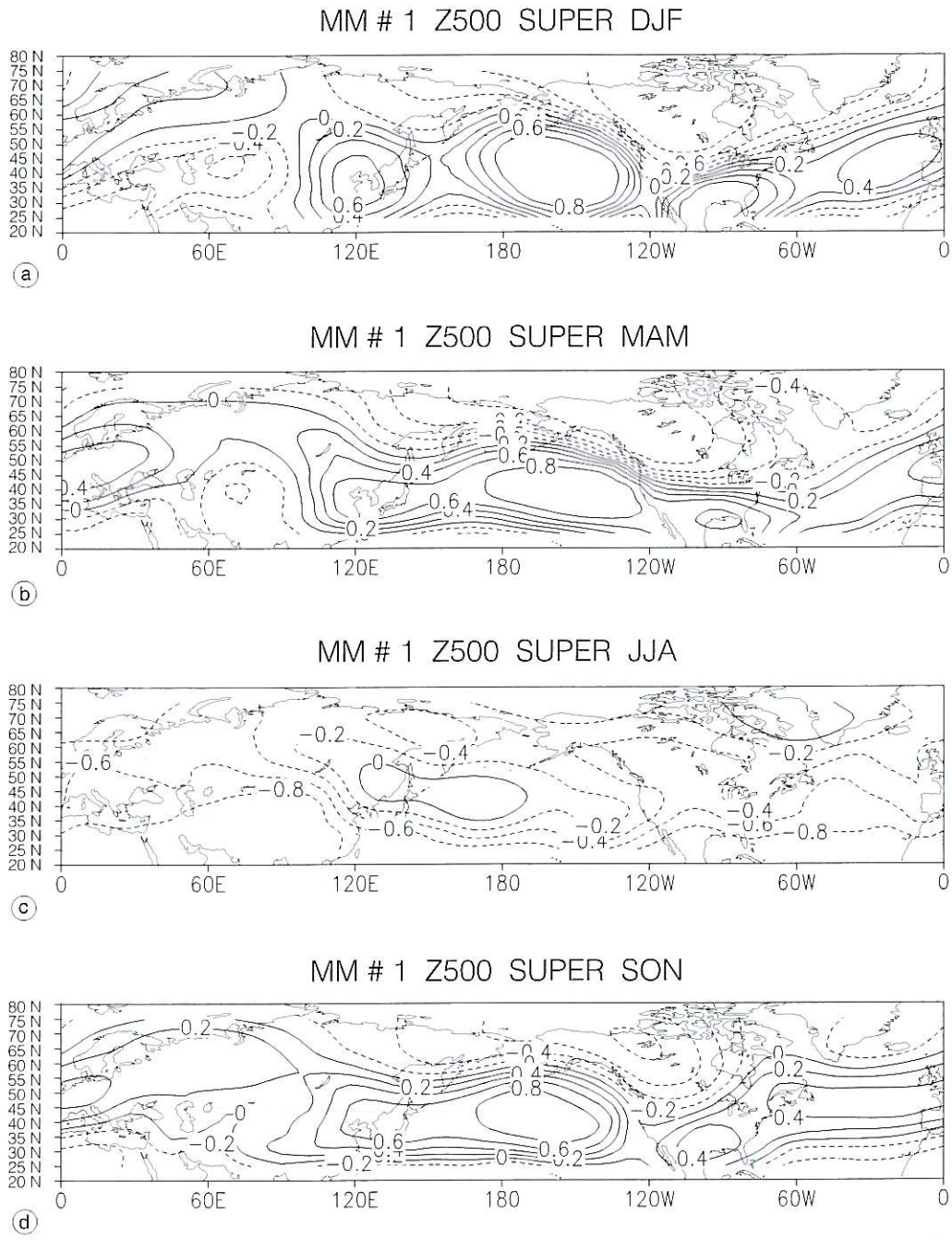

Fig. 7a-d. Same as fig. 6a-d except for Z500.

Table IV. Explained variance of the leading MM_m mode (computed as the weighted mean of the squared homogeneous correlations shown in figs. 6a-d and 7a-d) and SST-forced variance computed on the cross-validated time series of MM_m by the Rowell *et al.* (1995) formula.

	SLP (%)	Z500 (%)	SST-forced variance in SLP (%)	SST-forced variance in Z500 (%)
DJF	26	26.3	57.3	48.6
MAM	31.7	24.1	38.4	28.7
JJA	19.9	33	51.0	49.9
SON	18.6	16.8	39.3	22.7

most reproducible. This is the case in DJF, but not during the spring and autumn.

In DJF, there is a strong agreement between the OM_m and MM_m patterns for both fields (figs. 6a and 7a). The time series of MM_m remains highly related to Niño3.4 (respectively – 0.76 and – 0.85 for the leading MM mode of SLP and Z500), but the spread between the nine runs is not significantly related to the intensity of Niño3.4 SSTA (r between absolute values of Niño3.4 and standard deviation of the 9 runs = – 0.21 for SLP and 0.02 for Z500). The local explained variance by this mode in SLP reaches 50% over large areas in the North Pacific, but also over the North Atlantic from Florida to the Iberian peninsula (fig. 6a). The highest homogeneous correlations of Z500 are more concentrated around North America (fig. 7a). This mode is similar to the SST-forced ones found in Shukla *et al.* (2000) but is found here without removing the linear influence of the first EOF mode. Note that the spatial signature of this SST-forced mode is quite close to the usual definition of the NAO for SLP but not for Z500 (figs. 6a and 7a).

In MAM, the similarity between OM_m and MM_m is lower than in winter, especially for SLP (table III). This SST-forced mode is very close to its wintertime counterpart (figs. 6a,b and 7a,b), but the variance explained by SST drops to 29-38% (table IV) and the correlations with Niño3.4, albeit significant at the 0.05 level, reach only – 0.46 and – 0.76 respectively for SLP and Z500. The wintertime SST forcing on the extratropical circulation extends itself in spring. As in DJF, the spread is not significantly related to raw or absolute values of Niño3.4.

In JJA, the similarity between OM_m and MM_m patterns is strong for SLP but quite low for Z500. The SLP and Z500 MM_m patterns are quite similar (pattern correlation = 0.44). The new signal, exhibited by Z500 shows negative heterogeneous correlations over the subtropical area (with positive Z500 anomaly during warm Niño3.4 events). This relation is related to the anomalous warming (and then vertical expanse) of the tropical troposphere during ENSO events and also appears during the other seasons but is then dominated by the true extratropical pattern.

In SON, the OM_m and MM_m patterns are quite similar for SLP but not for Z500 (table IV). Both fields now exhibit basic pattern which is quite close to the winter and spring ones (figs. 6a-d and 7a-d). The SST-forced variance is decreased from the winter case, as during the spring.

5. Conclusions

Nine different runs issued from three different AGCMs were forced with the same SST and sea-ice conditions. The most skilful and most reproducible mode, independent from the initial conditions and the parametrizations used in each model, of sea level pressure and geopotential height at 500 hPa were extracted through SVD as in Moron *et al.* (1998) and Feddersen *et al.* (1998).

At hemispheric scale, the most reproducible in DJF, MAM and SON describes an extended PNA-like pattern. The exact difference between this SST-forced mode and the real PNA mode,

which is considered an internal mode of the atmosphere (Straus and Shukla, 2000; Shukla *et al.*, 2000) is beyond the scope of this paper. A new feature here is that it is found directly without removing the linear weight of the North Atlantic/Arctic oscillation as in Straus and Shukla (2000) and Shukla *et al.* (2000). This mode is also not confined around North America but has almost a hemispheric extent. This SST-forced is characterized by a very close pattern over the North Pacific and North America with just a weak eastward shift of the largest absolute SLP values relative to their Z500 counterpart. There are some differences outside this sector. Over the North Atlantic and Europe, the pattern resembles the NAO ones (Wallace and Gutzler, 1981; Barnston and Livezey, 1987) for SLP (with negative phase of the simulated NAO and reduced westerlies during the tropical Pacific warm events) but not exactly for Z500. This SST-forced mode does not really fit into the annular modes discussed elsewhere (*i.e.* Thompson and Wallace, 2000). This SST-forced mode is skilful in winter but not really in spring and not at all in autumn. It could suggest: i) that the SST forcing is relatively strong during the boreal winter season but not really in spring and not at all in autumn in the real atmosphere. In that case, the leading SST-forced mode remains almost unchanged from the autumn to the spring but its relative weight in the whole observed extratropical variance is weak in autumn and spring; ii) there are some systematic errors which appear clearly during the intermediate season. Another result is that this SST-forced mode is moderately to strongly related to Niño3.4 but that its full variability could not be explained by these regional SST indexes. It remains to be demonstrated from where exactly the SST forcing comes and if possible other sources of forcing, outside the tropical Pacific or even outside the tropical zone, are possible. The spread between the runs is not significantly related to the raw or absolute values of Niño3.4. In other words, this SST index seems, moderately to strongly related to the shift of the ensemble mean, but not to the spread amongst this ensemble. Future works should examine larger ensembles to dissect the two possible effects of a particular SST-forcing. Another interesting result of this study is the existence of a skilful and reproducible response in summer. This SST-forced response is stronger in SLP. The weights are now stronger over and around the North Pacific, with decreased (respectively increased) sea level pressure over (respectively around) the North Pacific during warm events. Further studies are warranted to test its importance in the North America summer variability.

Acknowledgements

The SLP data set used in this study was kindly provided by Tracy Basnett (UKMO, Bracknell). The runs were conducted under EC contract DICE-EV5V-CT94-0538 and the stay of one of us (VM) at IMGA was partially supported by this EC contract. Discussions with K. Miyakoda were also fruitful during the development of this work.

REFERENCES

BARNETT, T.P., K. ARPE, L.JI.M. BENGTSSON and A. KUMAR (1997): Potential predictability and AMIP implications of midlatitude climate variability in two general circulation models, *J. Climate*, **10**, 2321-2329.

BARNSTON, A.G. and R.E. LIVEZEY (1987): Classification, seasonality and persistence of low-frequency atmospheric circulation patterns, *M. Weather Rev.*, **115**, 1825-1850.

BJERKNES, J. (1964): Atlantic air-sea interaction, in *Advances in Geophysics* (Academic Press), vol. 10, 1-82.

DAVIES, J.R., D.P. ROWELL and C.K. FOLLAND (1997): North Atlantic and European seasonal predictability using an ensemble of multi-decadal AGCM simulations, *Int. J. Climatol.*, **17**, 1263-1280.

DAVIS, R. (1976): Predictability of sea surface temperature and sea surface pressure anomalies over the North Pacific Ocean, *J. Phys. Oceano.* **6**, 249-266.

DEQUÉ, M. and J. SERVAIN (1989): Teleconnections between tropical Atlantic sea surface temperatures and midlatitude 50 kPa heights during 1964-1986, *J. Climate*, **2**, 929-944.

FEDDERSEN, H. (2000): Impact of global sea surface temperature on summer and winter temperatures in Europe in a set of seasonal ensemble simulations, *Q. J. Meteorol. Soc.*, **126**, 2089-2109.

FEDDERSEN, H., A. NAVARRA and M.N. WARD (1999): A statistical correction approach for dynamical seasonal prediction, *J. Climate*, **12**, 1974-1989.

FRAEDRICH, K. (1990): European grosswetter during the warm and cold extremes of the El Niño Southern Oscillation, *Int. J. Climatol.*, **10**, 21-31.

FRAEDRICH, K. (1993): An ENSO impact on Europe? A review, *Tellus*, **46A**, 541-552.

FRAEDRICH, K. and K. MULLER (1992: Climate anomalies in Europe associated with ENSO extremes, *Int. J. Climatol.*, **12**, 25-31.

FRAEDRICH, K, K. MULLER and R. KUGLIN (1992): Northern Hemisphere circulation regimes during the extreme of the El Niño Southern Oscillation, *Tellus*, **44A**, 33-40.

GRAHAM, N.E., T.P. BARNETT, R. WILDE, U. SCHLESE and L. BENGTSSON (1994): On the roles of tropical and midlatitude SSTs in forcing interannual to onterdecadal variability in the winter Northern Hemisphere circulation, *J. Climate*, 7, 1416-1441.

GRÖTZNER, A., M. LATIF and T.P. BARNETT (1998): A decadal climate cycle in the North Atlantic Ocean as simulated by the ECHO coupled GCM, *J. Climate*, **11**, 831-847.

KHARIN, V.V. (1995): The relationship between sea surface temperature anomalies and atmospheric circulation in GCM experiments, *Climate Dyn.*, **11**, 359-375.

KRISHNAMURTI, T.N., C.M. KISHTAWAI, Z. ZHANG, T. LAROW, D. BACHIOCHI, E. WILLIFORD, S. GADGIL and S. SURENDRAN (2000): Multimodel ensemble forecasts for weather and seasonal climate, *J. Climate*, **13**, 4196-4216.

LAU, N.C. (1997): Interactions between Global SST anomalies and midlatitude atmospheric circulation, *Bull. Am. Meteorol. Soc.*, **78**, 21-34.

LAU, N.C. and M.J. NATH (1994): A modelling study of the relative roles of tropical and extratropical SST anomalies in the variability of the global atmosphere-ocean system, *J. Climate*, **7**, 1184-1207.

LAU, N.C. and M.J. NATH (1996): The role of «atmospheric bridge» in linking tropical Pacific ENSO events to extratropical SST anomalies, *J. Climate*, **9**, 2036-2057.

LIANG, X.Z., K.R. SPERBER, W.C. WANG and A.N. SAMUEL (1997): Predictability of SST forced climate signals in two atmospheric general circulation models, *Climate Dyn.*, **13**, 391-415.

LIVEZEY, R.E., A. LEETMA, M. MASUTANI, H.JI.M. RUI and A. KUMAR (1997): Teleconnective response of the Pacific/North American region atmosphere to large central equatorial Pacific SST anomalies, *J. Climate*, **10**, 1787-1820.

MORON, V. and M.N. WARD (1998): ENSO teleconnections with climate variability in the European and African sectors, *Weather*, **53**, 287-295.

MORON, V., A. NAVARRA , M.N. WARD and E. ROECKNER (1998): Skill and reproducibility of seasonal rainfall patterns in the tropics in ECHAM-4 GCM simulations with prescribed SST, *Climate Dyn.*, **14**, 83-100.

MORON, V., A. NAVARRA, M.N. WARD, C.K. FOLLAND, P. FRIEDERICHS, K. MAYNARD and J. POLCHER (2001): Analysing and combining atmospheric general circulation model simulations forced by prescribed SST: tropical response, *Ann. Geofis.*, **44** (4), 755-780 (this volume).

RENSHAW, A.C., D.P. ROWELL and C.K. FOLLAND (1998): Wintertime low-frequency weather variability in the North-Pacific American sector, *J. Climate*, **11**, 1073-1093.

ROWELL, D.P., C.K. FOLLAND, K. MASKELL and M.N. WARD (1995): Variability of the summer rainfall over tropical summer rainfall over tropical North Africa (1906-1992): observations and modelling, *Q. J. Meteorol. Soc.*, **121**, 669-704.

SARANAVAN, R. (1998): Atmospheric low-frequency variability and its relationship to mid-latitude SST variability: studies using the NCAR climate system community, *J. Climate*, **11**, 1386-1404.

SHUKLA, J., D.A. PAOLINO, D.M. STRAUS, D. DE WITT, M. FENNESSY, J.L. KINTER, L. MARX and R. MO (2000): Dynamical seasonal predictions with the COLA atmospheric model, *Q. J. Meteorol. Soc.*, **126**, 2265-2291.

STRAUS, D.M. and J. SHUKLA (2000): Distinguishing between the SST-forced variability and internal variability in mid-latitudes: analysis of observations and GCM simulations, *Q. J. Meteorol. Soc*, **126**, 2323-2350.

THOMPSON, D.W.J. and J.M. WALLACE (2000): Annular modes in the extratropical circulation. Part I: Month-to-month variability, *J. Climate*, **13**, 1000-1016.

VERBEEK, J. (1997): Wind-stress and SST variability in the North Atlantic area: observations and five coupled GCMs in concert, *M. Weather Rev.*, **125**, 942-956.

WALLACE, J.M. and D.S. GUTZLER (1981): Teleconnection in the geopotential height field during the Northern Hemisphere winter, *M. Weather Rev.*, **109**, 784-812.

WALLACE, J.M., C. SMITH and Q. JIANG (1990): Spatial patterns of atmosphere-ocean interaction in the northern winter, *J. Climate*, **3**, 990-998.

WALLACE, J.M., C. SMITH and C.S. BRETHERTON (1992): Singular value decomposition of wintertime sea surface temperature and 500-mb height anomalies, *J. Climate*, **5**, 561-576.

WARD, M.N. and A. NAVARRA (1997): Pattern analysis of ensemble GCM simulations with prescribed SST: boreal summer examples over Europe and the tropical Pacific, *J. Climate*, **10**, 2210-2220.

ZORITA, E. and C. FRANKIGNOUL (1997): Modes of North Atlantic decadal variability in the ECHAM1/LSG coupled ocean-atmosphere model, *J. Climate*, **10**, 183-200.

ZORITA, E., V.V. KHARIN and H. VON STORCH (1992): The atmospheric circulation and sea surface temperature in the North Atlantic area in winter: their interaction and relevance for Iberian precipitation, *J. Climate*, **5**, 1097-1108.

(received May 15, 2001;
accepted August 30, 2001)